

Synthesis and pharmacological activity of new carbonyl derivatives of 1-aryl-2-iminoimidazolidine

Part 1. Synthesis and pharmacological activity of chain derivatives of 1-aryl-2-iminoimidazolidine containing urea moiety

Dariusz Matosiuk^{a,*}, Sylwia Fidecka^b, Lucyna Antkiewicz-Michaluk^c, Izabela Dybała^d, Anna E. Koziol^d

^aDepartment of Synthesis and Technology of Drugs, Medical University, Staszica 6, PL-20-081 Lublin, Poland

^bDepartment of Pharmacodynamics, Medical University, Staszica 6, PL-20-081 Lublin, Poland

^cDepartment of Biochemistry, Institute of Pharmacology, Polish Academy of Sciences, Smętna 12, PL-31-343 Kraków, Poland

^dDepartment of Crystallography, Maria Curie-Skłodowska University, Maria Curie-Skłodowska Sq. 3, PL-20-031 Lublin, Poland

Received 26 February 2001; revised 31 July 2001; accepted 31 July 2001

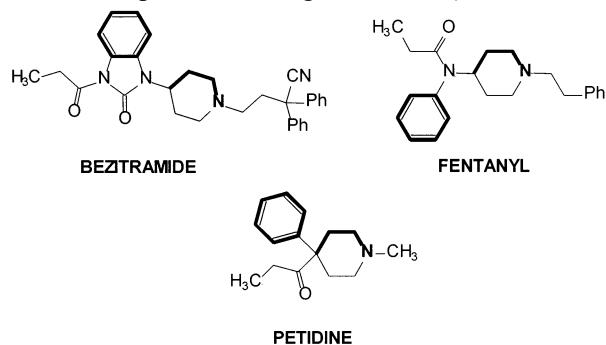
Abstract – The synthesis and physicochemical properties of new carbonyl derivatives of 1-aryl-2-iminoimidazolidine are presented. Isomeric 1-(1-arylimidazolidine-2-ylidene)-3-arylureas (series **A**) and 1-aryl-2-imine-3-arylaminocarbonylimidazolidines (series **B**) were obtained after the condensation reaction of 1-aryl-2-iminoimidazolidines and arylisocyanates. 1-Aryl-2-iminoimidazolidines were synthesised in a two-step reaction from the respective anilines. The molecular structure of 1-(1-phenylimidazolidine-2-ylidene)-3-(4-chlorophenyl)urea (**A2**) has been determined by X-ray crystallography. The representatives of both investigated series were evaluated in behavioural animal tests. They exhibited significant, especially analgesic, activity on the animal central nervous system (CNS). They displayed substantial effect on the serotonin and catecholamine neurotransmission as well, at very low toxicity (LD₅₀ over 2000 mg kg⁻¹ i.p.). In the binding affinity tests they exhibited moderate affinity (on the micromolar level) toward opioid (μ) and serotonin (5HT₂) receptors. The derivatives of series **A** had moderate affinity toward benzodiazepine (BZD) receptor as well. Distinctive differences observed in their activity spectra can be connected with the presence of particular structural features such as relative orientation of the two aromatic rings and the carbonyl moiety. © 2001 Éditions scientifiques et médicales Elsevier SAS

CNS activity / analgesic activity / non-peptoid opioids / μ opioid receptor pharmacophor model / X-ray structure analysis

1. Introduction

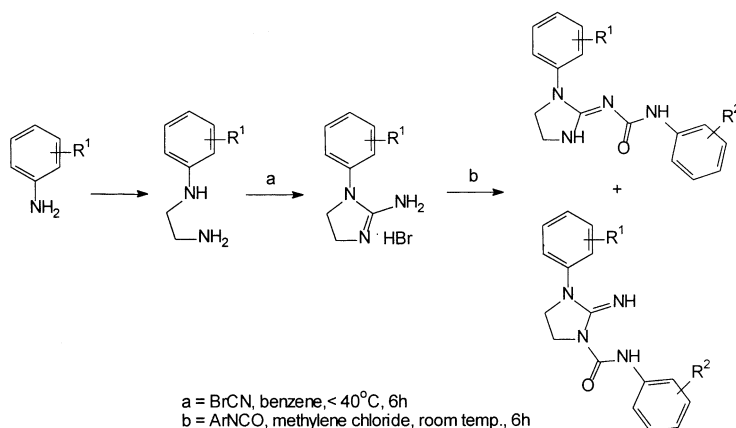
Many morphine-like narcotic analgesics bear in their structure similar features, which can play an important role in expressing their pharmacological activity. This is usually connected with the presence of the phenyl ring, tertiary nitrogen atom and the two-carbon fragment (e.g. as a part of the piperidine ring), which can be accommodated into the receptor cavity [1]. These features can be found in bezitramide, fentanyl and petidine, and their analogues. This ‘phar-

macophor’ model introduced by Beckett (with its further modifications [2–4]) was one of the first models used to explain the analgesic action (or its absence)



* Correspondence and reprints

E-mail address: darek@eskulap.am.lublin.pl (D. Matosiuk).



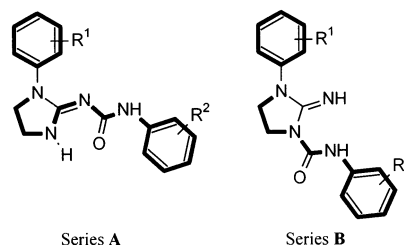
Scheme 1.

for morphine derivatives. It is still very useful for piperidine derivatives but does not pertain to the other active compounds, especially those without the basic nitrogen atom capable of creating a quaternary salt form.

In the recent years at the Department of Synthesis and Technology of Drugs, a number of simple and fused derivatives of imidazolidine was synthesised. In many cases [5] they exhibited analgesic activity, especially when the additional carbonyl group was present. To find out the part of their structure that can be a possible analgesic ‘pharmacophor’, a series of chain carbonyl derivatives of 1-aryl-2-iminoimidazolidine were synthesised.

It is worth noting that both the series differ only in the substitution place of the carbonyl group to the 1-arylimidazolidine nucleus. Analgesic activity ascertained in both of these groups suggests that the position of the carbonyl group is not as important for the

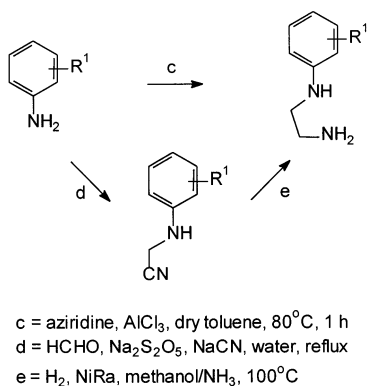
particular type of action as it probably plays a supporting role in binding, due to the high negative potential present on the oxygen atom. Some important role can be ascribed to the presence of the second aromatic ring as well.



2. Chemical part

The synthesis of the title carbonyl derivatives of 1-aryl-2-iminoimidazolidines was achieved by a sequence of reactions starting from the respective anilines (Scheme 1).

In the first step, anilines were converted into *N*-arylethylenediamines by the classical Knoevenagel and Mercklin method [6] (with Takeda modification [7]) or by the Lehmann method [8] (Scheme 2). Their further condensation with cyanogene bromide led to the formation of the hydrobromides of 1-aryl-2-aminoimidazolidines-2. In the earlier paper [9] the ability of 1-aryl-2-aminoimidazolidines-2 to undergo different nucleophilic substitution reactions on both, N3 and N6 nitrogen atoms, was presented. The results obtained allowed us to expect the formation of isomeric arylurea derivatives in the reaction of 1-aryl-2-aminoimidazolidines-2 with arylisocyanates as well.



Scheme 2.

Table I. Physicochemical properties of 1-(1-arylimidazolidine-2-ylidene)-3-aryl-urea (series **A**) and 1-aryl-2-imine-3-arylaminocarbonylimidazolidine derivatives (series **B**).

No.	R^1	R^2	R_f	M.p. (°C) ^a	Yield (%)
A1	H	H	0.36	168–169 (a)	64.2
A2	H	4-Cl	0.65	158–159 (b)	70.2
A3	H	3-Cl	0.35	137–138 (c)	69.5
A4	H	3,4-Cl ₂	0.54	160–162 (c)	63.1
A5	H	2,3-(–CH=) ₄	0.42	160–162 (a)	59.6
A6	4-CH ₃	H	0.49	178–180 (b)	57.7
A7	4-CH ₃	4-Cl	0.48	158–159 (b)	57.8
A8	4-CH ₃	3-Cl	0.58	142–143 (c)	42.7
A9	4-CH ₃	3,4-Cl ₂	0.49	167–169 (c)	62.6
A10	4-CH ₃	2,3-(–CH=) ₄	0.42	163–164 (a)	68.5
A11	4-Cl	H	0.38	159–161 (b)	62.6
A12	4-Cl	4-Cl	0.40	174–175 (b)	67.3
A13	4-Cl	3-Cl	0.48	129–130 (c)	64.5
A14	4-Cl	3,4-Cl ₂	0.49	187–189 (c)	63.4
A15	4-Cl	2,3-(–CH=) ₄	0.41	174–175 (a)	70.5
A16	4-CH ₃ O	H	0.47	138–140 (a)	64.4
A17	4-CH ₃ O	4-Cl	0.55	130–133 (b)	40.6
A18	4-CH ₃ O	3-Cl	0.63	144–145 (c)	66.7
A19	4-CH ₃ O	3,4-Cl ₂	0.61	127–128 (c)	69.1
A20	4-CH ₃ O	2,3-(–CH=) ₄	0.58	157–159 (a)	64.9
B1	H	H	0.44	184–185	27.2
B2	H	4-Cl	0.72	196–197	17.8
B3	H	3-Cl	0.49	163–164	23.9
B4	H	3,4-Cl ₂	0.60	180–182	25.5
B5	H	2,3-(–CH=) ₄	0.53	183–184	21.4
B6	4-CH ₃	H	0.47	195–197	24.3
B7	4-CH ₃	4-Cl	0.59	183–185	23.7
B8	4-CH ₃	3-Cl	0.70	167–169	27.7
B9	4-CH ₃	3,4-Cl ₂	0.59	187–188	19.5
B10	4-CH ₃	2,3-(–CH=) ₄	0.52	182–183	18.4
B11	4-Cl	H	0.54	179–180	32.3
B12	4-Cl	4-Cl	0.48	192–193	24.6
B13	4-Cl	3-Cl	0.58	150–151	19.9
B14	4-Cl	3,4-Cl ₂	0.59	199–201	20.2
B15	4-Cl	2,3-(–CH=) ₄	0.49	188–189	19.7
B16	4-CH ₃ O	H	0.62	158–160	12.3
B17	4-CH ₃ O	4-Cl	0.69	160–161	18.7
B18	4-CH ₃ O	3-Cl	0.68	154–155	16.7
B19	4-CH ₃ O	3,4-Cl ₂	0.70	167–168	19.4
B20	4-CH ₃ O	2,3-(–CH=) ₄	0.63	170–171	19.3

^a Solvent mixtures used for isolation of the crude reaction product.

Final products (compounds of series **A** and **B**) were separated by flash chromatography. The physicochemical data are presented in *table I*.

The **A** and **B** series compounds were identified by their ¹H-, ¹³C-NMR (*tables II and III*) and IR spectra. Additionally, structures of the series **A** derivatives were confirmed by the X-ray single-crystal analysis of **A2** (*table IV*).

In the ¹H-NMR spectra of the compounds of series

B, the C4 and C5 hydrogen atoms were presented as a broad singlet of the chemical shift value of ca. 4.0 ppm with a four hydrogen integration. The same hydrogen atoms in the compounds of the series **A** were represented by two double doublet signals of two hydrogen integration each at ca. 3.6 and 3.9 ppm, respectively, with the coupling constants of $J \sim 9$ Hz and $J' \sim 7.5$ Hz. The nitrogen-bonded hydrogen atoms in both series were present in the different

Table II. NMR data of 1-(1-arylimidazolidine-2-ylidene)-3-arylurea derivatives (series A).

No.	¹ H-NMR					¹³ C-NMR					
	N3 (s)	N8 (s)	C4/C5 (2 × dd, <i>J</i> (Hz))	Ar/Ar' (m)	C4	C5	Ar/Ar'		C=O	C=N	
A1	9.07	8.65	3.60/3.84 (<i>J</i> = 8.9, <i>J'</i> = 7.5)	7.10–7.80	45.3	40.0	120.0, 122.2, 125.4, 127.1, 127.4, 129.9, 130.3, 134.1, 134.7, 135.9		160.0	159.8	
A2	9.10	8.68	3.62/3.87 (<i>J</i> = 8.9, <i>J'</i> = 7.6)	7.10–7.75	45.3	39.9	120.4, 122.4, 124.8, 126.1, 127.8, 129.1, 130.2, 133.1, 137.4, 138.8		160.2	160.1	
A3	9.15	8.71	3.62/3.88 (<i>J</i> = 8.9, <i>J'</i> = 7.6)	7.15–7.75	45.7	40.0	121.1, 122.9, 123.7, 125.3, 126.4, 129.2, 132.2, 132.9, 136.4, 136.6		160.1	158.9	
A4	9.11	8.70	3.60/3.88 (<i>J</i> = 8.9, <i>J'</i> = 7.3)	7.10–7.80	45.5	40.0	120.9, 122.9, 125.4, 127.3, 130.8, 132.2, 136.2, 137.1, 137.6, 138.9		160.3	160.2	
A5	9.08	8.64	3.59/3.79 (<i>J</i> = 9.0, <i>J'</i> = 7.6)	7.05–7.85	45.6	40.0	119.6, 121.0, 124.5, 128.1, 132.2, 137.7, 140.2		160.1	160.0	
A6	9.05	8.62	3.61/3.80 (<i>J</i> = 8.8, <i>J'</i> = 7.6)	7.10–7.75	46.0	40.0	119.3, 120.9, 123.4, 126.1, 129.9, 131.2, 133.3, 135.9, 137.1, 138.1		160.1	160.1	
A7	9.06	8.63	3.62/3.85 (<i>J</i> = 8.8, <i>J'</i> = 7.5)	7.15–7.65	45.9	40.0	119.9, 121.4, 123.7, 124.9, 127.2, 129.9, 134.1, 136.3, 137.6, 139.0		160.3	159.8	
A8	9.12	8.67	3.61/3.88 (<i>J</i> = 8.8, <i>J'</i> = 7.5)	7.10–7.70	46.0	40.1	119.9, 121.9, 124.0, 125.3, 129.1, 129.7, 130.7, 133.2, 133.9, 136.9		160.2	159.8	
A9	9.11	8.68	3.63/3.86 (<i>J</i> = 8.9, <i>J'</i> = 7.4)	7.10–7.80	46.0	40.0	120.2, 122.3, 124.1, 125.5, 126.8, 128.3, 132.7, 137.1, 138.6, 140.1		160.4	160.0	
A10	9.04	8.64	3.62/3.85 (<i>J</i> = 9.0, <i>J'</i> = 7.4)	7.10–7.90	45.7	40.1	119.1, 121.8, 123.3, 125.7, 127.3, 132.2, 135.4, 137.4, 139.9		160.0	159.3	
A11	9.10	8.61	3.62/3.83 (<i>J</i> = 9.0, <i>J'</i> = 7.5)	7.10–7.65	46.2	40.1	121.4, 122.7, 124.7, 125.7, 127.3, 127.7, 130.1, 136.1, 138.2, 140.7		160.5	160.0	
A12	9.16	8.58	3.64/3.84 (<i>J</i> = 8.9, <i>J'</i> = 7.5)	7.20–7.65	46.3	40.0	120.9, 122.8, 124.1, 126.3, 127.8, 130.2, 131.0, 133.1, 137.9, 140.3		160.6	160.2	
A13	9.17	8.68	3.65/3.86 (<i>J</i> = 9.0, <i>J'</i> = 7.5)	7.15–7.75	46.0	40.0	121.2, 123.4, 125.3, 127.8, 128.0, 132.7, 133.1, 136.9, 139.1, 140.1		160.2	160.1	
A14	9.19	8.64	3.63/3.84 (<i>J</i> = 8.9, <i>J'</i> = 7.)	7.05–7.90	46.0	39.8	121.7, 123.9, 125.9, 127.9, 129.8, 130.1, 131.7, 134.0, 138.7, 140.9		160.4	160.1	
A15	9.10	8.66	3.61/3.83 (<i>J</i> = 8.9, <i>J'</i> = 7.5)	7.10–7.75	46.1	39.9	120.1, 123.0, 125.6, 126.5, 127.9, 130.2, 135.2, 138.3, 141.2		160.4	160.0	
A16	9.05	8.61	3.59/3.77 (<i>J</i> = 8.9, <i>J'</i> = 7.4)	7.15–7.65	45.8	40.0	120.1, 122.7, 127.3, 127.8, 128.3, 129.1, 130.1, 130.9, 135.0, 139.6		160.1	159.9	
A17	9.09	8.64	3.63/3.83 (<i>J</i> = 8.9, <i>J'</i> = 7.4)	7.10–7.70	45.9	40.0	120.4, 121.9, 124.2, 126.6, 128.0, 129.2, 132.7, 134.1, 136.0, 140.3		160.3	160.0	
A18	9.13	8.68	3.63/3.85 (<i>J</i> = 8.9, <i>J'</i> = 7.6)	7.10–7.75	45.9	39.9	120.3, 123.5, 125.2, 126.9, 127.3, 128.9, 131.9, 132.2, 137.2, 139.2		160.1	160.0	
A19	9.12	8.68	3.61/3.86 (<i>J</i> = 9.1, <i>J'</i> = 7.6)	7.10–7.80	45.7	40.1	120.7, 121.2, 123.9, 127.1, 127.9, 130.7, 134.7, 137.3, 137.9, 142.3		160.2	160.1	
A20	9.03	8.65	3.60/3.81 (<i>J</i> = 8.9, <i>J'</i> = 7.5)	7.00–7.85	45.9	40.1	118.7, 120.7, 121.9, 123.2, 126.9, 130.7, 133.1, 135.4, 137.3, 140.9		160.3	160.0	

regions of the spectra. In series **A**, the N3 and N8 hydrogen atom signals were located close to each other at ca. 8.6 and 9.0 ppm, respectively. The N6 and N8 hydrogen atom signals of series **B** were shifted down to the lower field spectra and occurred at ca. 9.6 and 11.6 ppm, respectively.

The ^{13}C -NMR spectra of series **A** and **B** derivatives revealed major differences in the chemical shifts of the carbonyl (C=O) and carbimino (C=N) carbon atoms.

In series **A**, they were observed at ca. 162 and 160 ppm, whereas in series **B**, at ca. 155 and 150 ppm, respectively. The signals of the C4 and C5 carbon atoms have had similar chemical shift values in both the series of compounds—40 ppm (C5) and 46 ppm (C4) for **A**; and 41 ppm (C5) and 48 ppm (C4) for **B**.

The IR spectra confirm the structure of the compounds investigated. The C=NH absorption bands (~ 3410 , $\sim 1640\text{ cm}^{-1}$) were present only in the spec-

Table III. NMR data of 1-aryl-2-imine-3-arylamino-carbonylimidazolidine derivatives (series **B**).

No.	^1H -NMR				^{13}C -NMR							
	N6 (s)	N8 (s)	C4/C5 (bs)	Ar/Ar' (m)	C4	C5	Ar/Ar'				C=O	150.0
B1	11.47	9.65	4.02	7.10–7.65	47.5	41.1	116.7, 124.4, 126.6, 128.3, 128.8, 133.3, 134.9, 136.2, 137.8				154.9	150.0
B2	11.43	9.78	4.03	7.05–7.75	47.7	41.0	119.4, 122.9, 125.7, 127.3, 128.1, 130.2, 136.3, 139.1, 139.9				154.7	150.3
B3	11.70	9.77	4.04	6.90–7.75	47.7	41.0	118.9, 123.4, 126.7, 126.9, 129.2, 130.7, 134.5, 136.4, 137.4				155.2	150.0
B4	11.65	9.73	4.02	7.05–7.75	47.5	41.2	118.3, 120.9, 125.1, 127.2, 129.2, 133.7, 135.0, 137.5, 139.1				155.1	150.1
B5	11.57	9.69	4.02	7.00–7.70	47.5	41.1	119.6, 121.0, 124.5, 128.1, 132.2, 137.7, 140.2				155.0	150.0
B6	11.31	9.64	4.01	7.05–7.60	47.9	41.0	119.3, 120.7, 124.7, 127.4, 128.2, 130.2, 133.7, 135.1, 137.0, 139.3				154.9	150.6
B7	11.68	9.69	4.00	7.05–7.70	47.8	41.0	120.7, 121.4, 123.3, 126.9, 127.8, 129.4, 131.6, 137.0, 138.5, 139.9				154.9	150.6
B8	11.69	9.71	4.04	7.00–7.75	47.9	41.2	120.4, 121.8, 123.9, 126.8, 128.9, 129.2, 131.2, 136.6, 138.6, 139.2				155.3	150.3
B9	11.54	9.73	4.06	6.95–7.75	47.9	41.3	120.9, 122.2, 125.1, 128.0, 128.8, 129.6, 135.1, 136.1, 137.3, 140.7				155.1	150.0
B10	11.43	9.69	4.01	7.00–7.75	47.6	41.3	119.9, 121.6, 123.3, 125.5, 126.5, 129.2, 130.4, 135.5, 139.8				155.2	150.1
B11	11.39	9.70	4.03	7.10–7.75	47.5	41.2	120.7, 123.2, 125.0, 126.3, 129.1, 129.9, 133.4, 135.4, 137.2, 139.9				155.2	150.5
B12	11.79	9.72	4.04	7.10–7.60	47.7	41.0	121.5, 122.2, 123.7, 127.7, 128.2, 130.1, 132.2, 136.4, 138.9, 140.7				155.3	150.7
B13	11.74	9.69	4.04	7.00–7.65	47.9	41.1	121.3, 122.7, 124.3, 126.2, 127.0, 128.2, 131.1, 135.9, 138.3, 141.5				155.5	150.2
B14	11.62	9.73	4.06	7.00–7.75	48.0	40.9	120.9, 123.6, 124.9, 126.9, 127.7, 129.1, 134.7, 137.8, 138.5, 142.8				155.2	150.3
B15	11.55	9.66	4.03	6.95–7.75	47.7	41.0	120.7, 122.9, 123.9, 126.6, 129.0, 130.1, 134.3, 136.8, 141.8				155.0	150.0
B16	11.47	9.54	4.01	7.05–7.75	47.7	41.0	119.9, 120.9, 124.7, 125.3, 126.8, 128.7, 131.3, 135.3, 139.2, 140.7				155.2	150.0
B17	11.58	9.59	4.04	7.05–7.70	47.8	41.3	118.8, 120.6, 124.1, 128.0, 128.3, 129.2, 133.4, 136.8, 138.7, 142.2				155.0	150.2
B18	11.63	9.62	4.06	7.05–7.80	47.6	41.3	120.1, 121.9, 124.7, 128.1, 128.6, 129.1, 132.9, 136.7, 138.9, 140.9				155.1	150.3
B19	11.60	9.66	4.07	7.00–7.80	47.9	41.1	120.8, 122.3, 124.9, 127.1, 128.2, 128.7, 132.5, 135.5, 139.5, 141.4				155.3	150.1
B20	11.51	9.61	4.05	7.00–7.80	47.7	41.2	120.5, 121.1, 123.3, 125.9, 127.2, 130.3, 131.9, 138.8, 141.7				154.9	149.7

Table IV. Atomic coordinates ($\times 10^4$) and equivalent isotropic displacement parameters ($\text{\AA}^2 \times 10^3$) for **A2**.

	<i>x</i>	<i>y</i>	<i>z</i>	<i>U</i> (eq)
N(1)	5394(1)	3419(1)	−2487(1)	40(1)
C(2)	5546(2)	4423(1)	−2084(1)	38(1)
N(3)	4738(2)	5434(1)	−2469(1)	49(1)
C(4)	4133(2)	5195(2)	−3277(2)	55(1)
C(5)	4348(2)	3783(2)	−3120(1)	48(1)
N(6)	6316(2)	4326(1)	−1401(1)	45(1)
C(7)	6503(2)	5406(2)	−1135(1)	42(1)
O(7)	6280(1)	6476(1)	−1601(1)	53(1)
N(8)	7059(2)	5152(1)	−256(1)	54(1)
C(9)	7454(2)	5993(2)	241(1)	42(1)
C(10)	8441(2)	5526(2)	844(1)	51(1)
C(11)	8863(2)	6300(2)	1364(1)	50(1)
C(12)	8293(2)	7542(2)	1279(1)	43(1)
C(13)	7318(2)	8023(2)	685(1)	45(1)
C(14)	6894(2)	7246(2)	168(1)	45(1)
Cl(1)	8811(1)	8526(1)	1935(1)	66(1)
C(15)	6040(2)	2169(1)	−2290(1)	37(1)
C(16)	7284(2)	1851(2)	−2008(1)	46(1)
C(17)	7894(2)	617(2)	−1847(2)	54(1)
C(18)	7298(2)	−326(2)	−1980(1)	53(1)
C(19)	6081(2)	−15(2)	−2277(2)	53(1)
C(20)	5445(2)	1216(2)	−2430(1)	46(1)
N(1A)	2469(1)	8648(1)	−3542(1)	42(1)
C(2A)	3675(2)	8524(1)	−4121(1)	36(1)
N(3A)	3521(2)	8908(2)	−5095(1)	51(1)
C(4A)	2189(2)	9377(2)	−5258(1)	51(1)
C(5A)	1449(2)	9119(2)	−4192(1)	48(1)
N(6A)	4755(1)	8058(1)	−3723(1)	40(1)
C(7A)	5903(2)	7947(2)	−4385(1)	39(1)
O(7A)	6054(1)	8277(1)	−5315(1)	59(1)
N(8A)	6928(1)	7393(1)	−3861(1)	43(1)
C(9A)	8236(2)	7051(2)	−4261(1)	40(1)
C(10A)	9084(2)	6379(2)	−3589(1)	50(1)
C(11A)	10 385(2)	5990(2)	−3926(1)	54(1)
C(12A)	10 858(2)	6274(2)	−4941(1)	47(1)
C(13A)	10 043(2)	6947(2)	−5616(1)	51(1)
C(14A)	8735(2)	7337(2)	−5283(1)	50(1)
Cl(1A)	12 492(1)	5792(1)	−5389(1)	67(1)
C(15A)	2161(2)	8374(1)	−2472(1)	37(1)
C(16A)	3045(2)	8307(2)	−1802(1)	47(1)
C(17A)	2670(2)	8094(2)	−760(1)	53(1)
C(18A)	1419(2)	7954(2)	−364(1)	53(1)
C(19A)	546(2)	8005(2)	−1021(1)	54(1)
C(20A)	905(2)	8209(2)	−2066(1)	46(1)

U(eq) is defined as one-third of the trace of the orthogonalised U_{ij} tensor.

tra of series **B** derivatives. Series **A** compounds could be recognised by the presence of the specific absorption bands of the C=N– and secondary >NH bonds, respectively, at ~ 3300 and ~ 1590 cm^{-1} . The spectra

of both series exhibited a similar absorption for NH–Ar (~ 3445 cm^{-1}) and C=O amidic (3308–3356 and ~ 1620 cm^{-1}) fragments typical of the urea derivatives, as well as secondary and tertiary amidic bands (N–H and C–N) at ~ 1515 , 1321 and 1238 cm^{-1} .

The spectral data (^1H -NMR, IR) and X-ray crystallography confirmed that compounds of series **A** can predominantly exist in the tautomeric imino form.

3. Crystallographic part

Two symmetrically independent molecules of **A2** are observed in its crystal structure. They are connected by two intermolecular hydrogen bonds (N3–H \cdots N6a and N8a–H \cdots O7) to form the dimer (*figure 1*). The imidazolidine ring in both the molecules is nearly planar and in the urea moiety it is completely flat. The planes of these fragments in the first molecule form an angle of about 20° , whereas in the second molecule they are nearly coplanar (the respective angle is 4°). The conformations are stabilised by the same kind of intramolecular hydrogen bond, i.e. between imidazolidine N3–H and urea carbonyl O7 atoms (N3–H \cdots O7 and N3a–H \cdots O7a) (*figure 2*).

4. Pharmacological part

4.1. Behavioural tests

Acute toxicity of the compounds tested (**A2**, **A3**, **A5**, **A7**, **A8** and **B7**) was lower than 2000 mg kg^{-1} i.p. and therefore $\text{LD}_{50} = 2000$ mg kg^{-1} was accepted for further studies. High doses of the compounds investigated induced sedation, noticeable hypothermia and decreased responsiveness to external stimuli.

The depressive action on the spontaneous locomotor activity in mice was observed after the administration of all compounds (doses of 0.1 and 0.05 LD_{50} inhibited the activity significantly). A slightly weaker decrease in activity in mice was produced by **A3** (significant only after 0.1 LD_{50}) (*figure 3*).

Almost all substances (except **A2**, **A3**) prolonged the hexobarbital narcosis significantly (data not presented).

Body temperature of normothermic mice was lowered significantly (in 60 and/or 90 min of study) by all the compounds tested (*figure 4*).

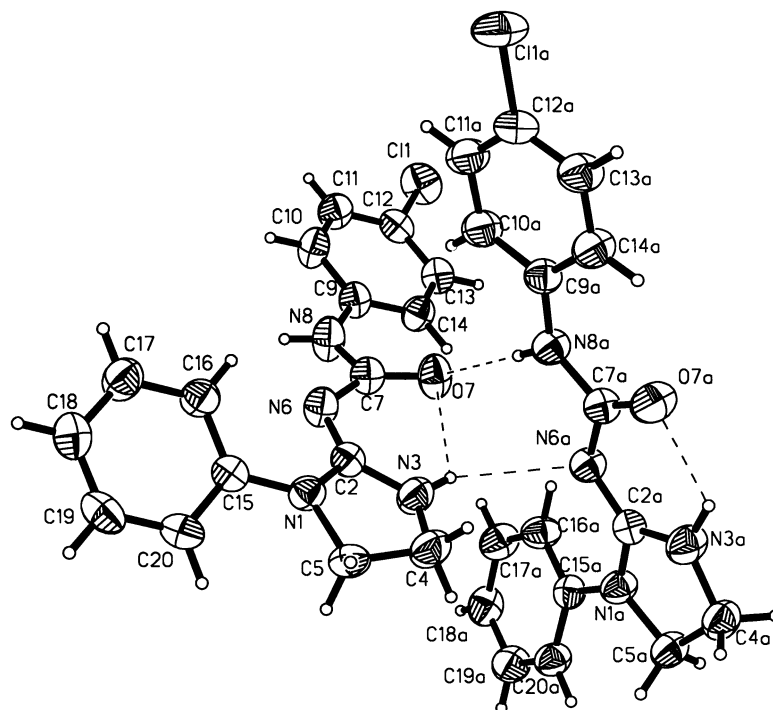


Figure 1. Perspective view of the two crystallographically independent **A2** molecules with atom numbering. Hydrogen bonds are represented by dashed lines. Geometry of intramolecular hydrogen bonds: N3···O7 2.708(2) Å; N3–H3n 0.86 Å; H3n···O7 2.25 Å; \angle N3–H3n···O7 113° and N3a···O7a 2.612(2) Å; N3a–H3na 0.86 Å; H3na···O7a 2.05 Å; \angle N3a–H3na···O7a 122°. Geometry of intermolecular hydrogen bonds: N3···N6a 3.090(2) Å; N3–H3n 0.86 Å; H3n···N6a 2.63 Å; \angle N3–H3n···N6a 114° and N8a···O7 3.037(2) Å; N8a–H8na 0.86 Å; H8na···O7 2.19 Å; \angle N8a–H8na···O7 169°.

Pentylenetetrazol-induced seizures were not changed by the substances investigated (data not presented).

In the ‘hot plate’ test, the compounds investigated given in a dose of 200 mg kg^{−1} (0.1 LD₅₀) prolonged the response to thermal stimuli in mice significantly, except for compound **A4**, which did not produce the effect (data not presented). The potent antinociceptive activity of all compounds was observed in the ‘writhing test’ in mice (figure 5). Naloxone (5 mg kg^{−1}) reversed the antinociceptive effect of **A5**, **A8** and **B7** significantly, and attenuated that of **A2** markedly but not significantly (figure 6).

The motor coordination, measured in mice in rotarod test, was not impaired by the compounds tested.

Amphetamine hyperactivity was increased significantly by **A2**, **A3** and **B7**, and markedly but not significantly by **A5**, **A7** and **A8** (figure 7).

The head-twitch responses to 5-HTP were abolished by **A8** and **B7**, decreased significantly by **A2** and **A5**, and not attenuated significantly by **A3** and **A7** (figure 8).

4.2. Receptors affinity tests

The two compounds, **A5** and **B7**, exhibiting the highest activity in the behavioural tests, representatives of both investigated series, were subjected to the binding

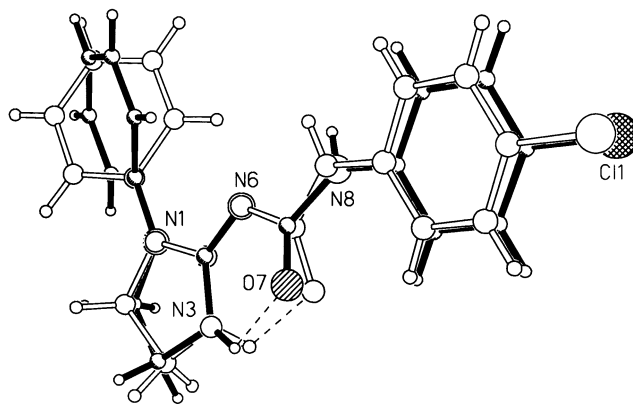


Figure 2. Comparison of two conformations adopted by symmetrically independent molecules of **A2** in the crystal.

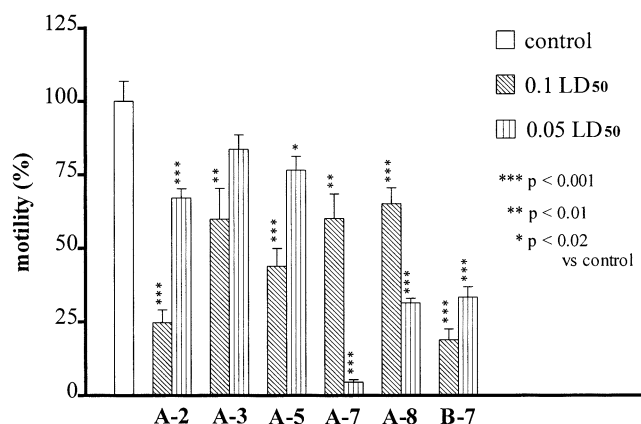


Figure 3. The influence of the tested compounds (A2, A3, A5, A7, A8 and B7) on the spontaneous locomotor activity of mice. Note: number of movements in the control groups was 237–305 (= 100%). The results are expressed as the mean \pm SEM for a group of ten mice.

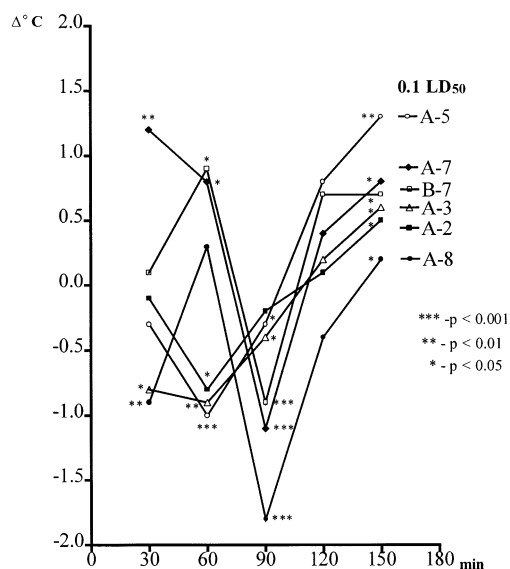


Figure 4. The influence of the tested compounds on the body temperature of mice. Note: each point represents the mean for a group of ten mice.

affinity tests. Three types of receptors were investigated: an opioid receptor (type μ); a serotonin receptor (5-HT₂); and a benzodiazepine receptor (BZD). Radioligand displacement method was applied. Selective antagonists were used for each receptor: Naloxone in the presence of sodium ions for the opioid μ receptor; Ketanserin for the 5-HT₂ receptor; and Flunitrazepam for the BZD receptor. The affinity was calculated as

EC₅₀ values and the results are presented in table V. The specific binding represented by displacement curves is presented in figures 9–11.

The A5 compound exhibited micromolar binding affinity toward all the three receptors. The B7 compound exhibited micromolar binding affinity only toward opioid and serotonin receptor.

The affinity toward the μ receptor was expressed to be stronger than the affinity toward serotonin. For the A5 compound, the EC₅₀ values of opioid and BZD receptors were almost the same (7.0 and 9.8, respectively) and about twofold higher than 5-HT₂ (16.0 μ mol).

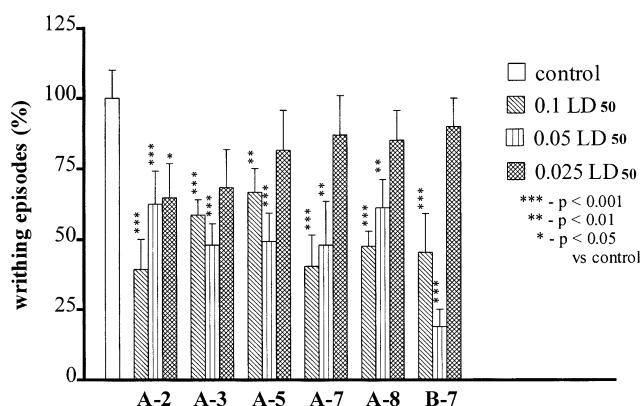


Figure 5. The antinociceptive effects of the tested compounds in the writhing test in mice. Note: number of writhing episodes in the control groups was 26–35 (= 100%). The results are expressed as means \pm SEM of a group of eight mice.

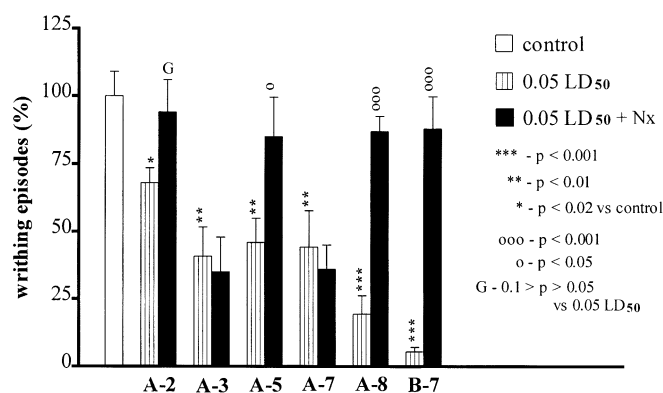


Figure 6. The influence of naloxone (Nx), 5 mg kg⁻¹ s.c., on the antinociceptive activity of the tested compounds in the writhing test. Note: number of writhing episodes of control mice was 22–32 (= 100%). The results are expressed as mean \pm SEM of a group of eight mice.

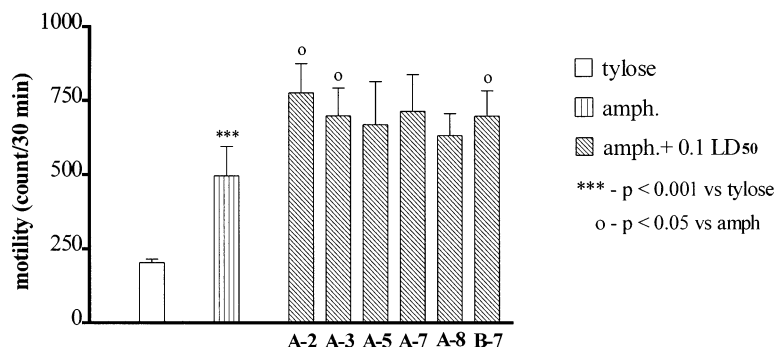


Figure 7. The influence of the tested compounds on amphetamine (amph) (5 mg kg^{-1})-induced hyperactivity of mice. Note: the results are expressed as mean \pm SEM of a group of ten mice.

5. Results and discussion

The results of the pharmacological investigation showed that both the investigated series exerted significant influence on the central nervous system (CNS) of laboratory animals. The most important seems to be their strong CNS depressive and antinociceptive effects.

The depressant action was expressed in the decrease of the spontaneous motility, lowering of the body temperature and prolongation of the hexobarbital induced narcosis. In other tests, they revealed the influence on the neurotransmission of catecholamines by affecting both the serotonin (reducing 'head twitch' responses after 5-HTP administration) and dopamine (increase of amphetamine induced hyperactivity) pathways. The influence on the serotonin pathway was confirmed in the binding assay test.

The highly significant antinociceptive activity was confirmed both in the 'writhing' test, reversible at a small dose of naloxone and in the binding assay test.

During the behavioural tests, no respiratory problems were observed (data not presented). This observation seems to be important because the compounds investigated having an affinity toward the opioid system could be devoid of the side effects typical for the other opioid ligands.

As a principle of common theories and models for the activation of CNS receptors (particularly the opioid and serotonin receptors) presence of the basic nitrogen atom seems to be essential for binding the endogenous drug molecules to the receptor [10, 11].

Although a serotonergic activity observed in both series can be explained by the presence of the urea moiety [12], the strong opioid action is not explain-

able in the view of the commonly used pharmacophor models. The compounds investigated can be considered as oxo derivatives of guanidine or guanyl deriva-

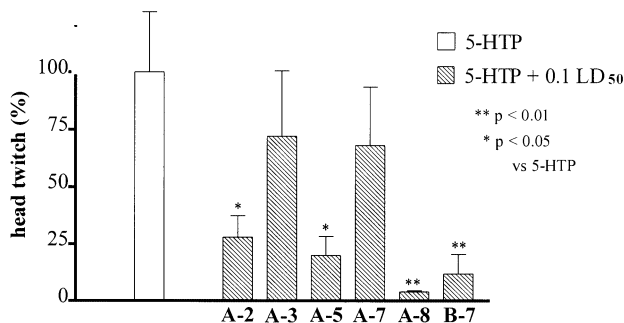


Figure 8. The influence of the tested compounds on the head twitch responses evoked by 5-hydroxytryptophan (5-HTP) (180 mg kg^{-1}). Note: number of 'head twitch' in the control group was 11.5 (= 100%). The results are expressed as mean \pm SEM of a group of eight mice.

Table V. EC_{50} values (μmol) in binding tests of compounds **A5** and **B7** on opioid (μ), serotonin (5-HT₂) and BZD receptors.

	μ	5-HT ₂	BZD
Naloxone	0.013		
Morphine	0.20		
Ketanserin		0.002	
Serotonin		1.90	
Clonazepam			0.001
Diazepam			0.005
A5	7.0	16.0	9.8
B7	1.0	13.0	> 100

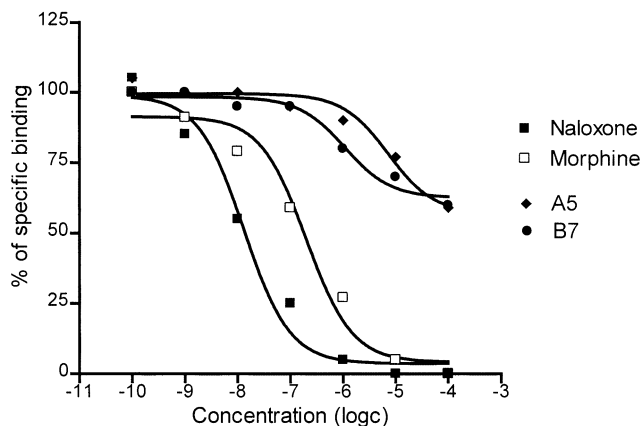


Figure 9. Displacement of ³H-Naloxone from its binding sites by investigated compounds (A5 and B7) (μ opioid receptor- limbic forebrain).

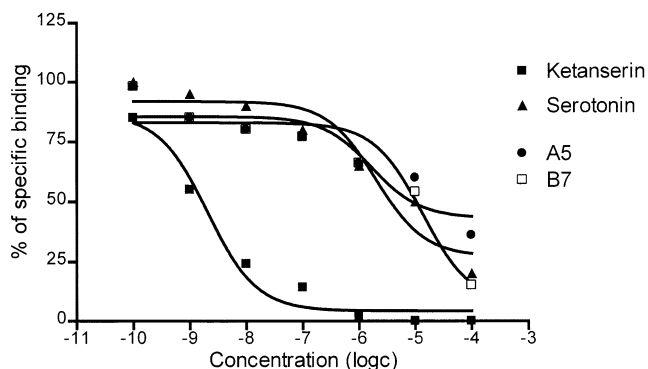


Figure 10. Displacement of ³H-Ketanserin from its binding sites by investigated compounds (A5 and B7) (5-HT₂ receptor).

tives of urea. It is known from the literature that neither of them is able to form stable cations; therefore the guanidine moiety cannot be taken into account for any ionic interactions within the receptor active domain. So far, publications concerning the significant opioid activity of derivatives deprived of the basic nucleus are scarce in the scientific literature. From this point of view the results of our investigation would give an interesting intake into the theory of drug–receptor interactions and suggest that the presence of the proton acceptor site (nitrogen atom) in the structure of the potential ligands of the opioid receptors would not be a strict prerequisite for the activity.

The shape of the replacement curves in the opioid receptor binding assay test can suggest that the investigated derivatives can act as partial agonists and

competitive antagonists as well. Although the antagonist activity was not confirmed thoroughly in the pharmacological tests, this possibility could not be excluded, especially based on the structural analysis of the most preferable conformers for both series.

Among the three common features found in the structure of most of the biologically active compounds responsible for the binding and activation of certain proteins (ionic, polar-H-bond type and hydrophobic interactions) in the structure of series A and B compounds, only two are present.

The two aromatic rings form two hydrophobic fragments located at the opposite sites of the molecules able to interact with the respective hydrophobic pockets in the receptor domain. The second feature present in the structure of the compounds investigated is the polar, carbonyl C=O group of the urea moiety. The oxygen atom of this group having a high electron net-charge collected on it can be a strong H-bond acceptor site. This kind of interaction usually anchors compounds into the receptor active site, causing its blocking or activation.

Similar features can be found in the molecules of the typical opioid receptors' ligands despite their different molecular structure. Measurements of the distances and angles between the aromatic rings and polar C=O group (*table VI*) prove the importance of these three fragments and their respective location in the opioid receptors' excitation. They fit a triangle, the sides and angles of which forms a new, non-classical pharmacophor model of the μ receptor activation (*figure 12*).

The observed and calculated distances Ar¹–Ar² (*b*) and Ar¹–O (carbonyl) (*a*) in the crystal and the predicted conformer **1** of A2, A5 and B7 are similar to the respective distances in the selected ligands of the opioid receptors (*figures 2 and 12, table VI*). There are some differences in the distances between the second aromatic ring (or other hydrophobic substituents) (Ar²) and the carbonyl group (*c*), and the angles defining the location of both the aromatic rings in comparison to the oxo moiety (*ab* and *ac*). In the active ligands (Bezitramide, Fentanyl, SNC-80) the (*c*) distance is about 11 Å and the respective angles are acute (60–90°), while in the conformers **1** the distance is about 7 Å and angles unequal (*ac*—ca. 120°; *ab*—ca. 40°).

The shortening of the distance (*c*) could be responsible for the weaker activity of A5 and B7 in comparison to the reference compounds (e.g. morphine or fentanyl).

The structure of the series **A** and **B** derivatives is flexible and allows free rotation on the C–N bonds of the urea moiety. Three distinct conformers can be attained for each series. Conformers **2** and **3** have a different dimension of the Ar¹–Ar²–O triangle due to the difference in the location of the respective aromatic rings (*figure 13*). Comparison of distances and angles in conformers **2** with the μ receptor specific antagonist—naltrexone shows that the respective di-

mensions are almost the same. The energy difference between the conformers does not exceed 30 kcal mol⁻¹ ($\Delta E_{2A5-1A5} = 7.79$ kcal mol⁻¹, $\Delta E_{3A5-1A5} = 16.68$ kcal mol⁻¹, $\Delta E_{2B7-1B7} = 20.09$ kcal mol⁻¹, $\Delta E_{3B7-1B7} = 28.05$ kcal mol⁻¹), which means that the compounds can achieve both the agonist and antagonist conformations easily [10]. This suggests that the compounds investigated can act as partial agonists and it is also possible that at least some number of

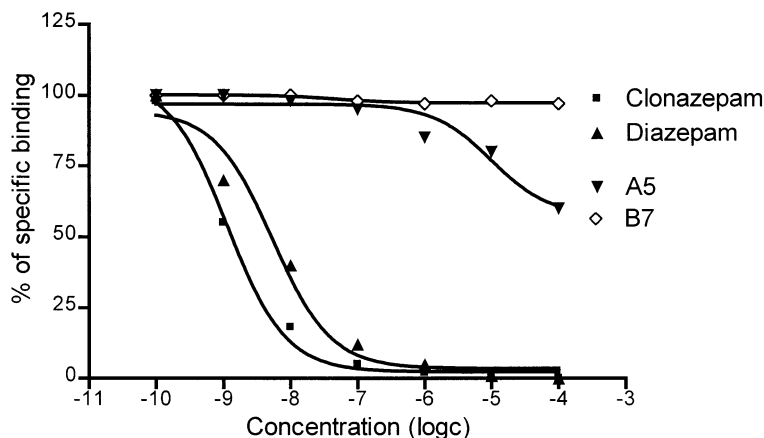


Figure 11. Displacement of ³H-Flunitrazepam from its binding sites by investigated compounds (**A5** and **B7**) (BZD—benzodiazepine receptor).

Table VI. Observed and calculated distances and angles between aromatic rings and oxo-group in compounds of series **A** and **B**, and selected ligands of opioid receptors.

		Distances (Å)			Angles (°)		
		<i>a</i>	<i>b</i>	<i>c</i>	<i>ac</i>	<i>ab</i>	<i>bc</i>
A2	crystal (A2) ^a	3.95	8.57	6.25	111	43	26
		3.97	8.59	6.32	112		25
	conformer 1	4.0	8.6	6.0	117	38	25
A5	conformer 1	4.8	8.6	6.4	98	48	34
	conformer 2	6.0	5.6	6.1	55	65	60
	conformer 3	5.2	7.4	5.9	82	53	45
B7	conformer 1	3.9	9.0	7.1	110	45	25
	conformer 2	5.1	6.6	7.4	60	77	43
	conformer 3	3.8	9.3	7.0	113	44	23
Bezitramide	local minimum energy conformer	4.6	10.5	11.4	67	89	24
Fentanyl		4.8	10.4	10.6	77	77	26
Petidine ^b		4.4	5.9	6.9	59	82	39
SNC-80		8.3	8.9	11.8	50	84	46
Naltrexone ^b		5.4	6.4	7.8	82	43	55

Energy optimisation performed by PC Spartan Pro [13], ab initio module, RHF approximation, 3-21G(*) basis set.

^a Values for two symmetrically independent molecules present in the crystal.

^b Second aromatic ring is replaced by a hydrophobic methyl (Petidine) or cyclopropylmethyl (Naltrexone) moieties.

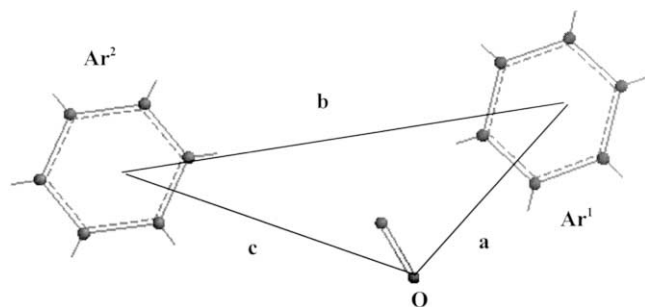


Figure 12. Intramolecular distances and angles in the proposed pharmacophor of series **A** and **B** opioid activity.

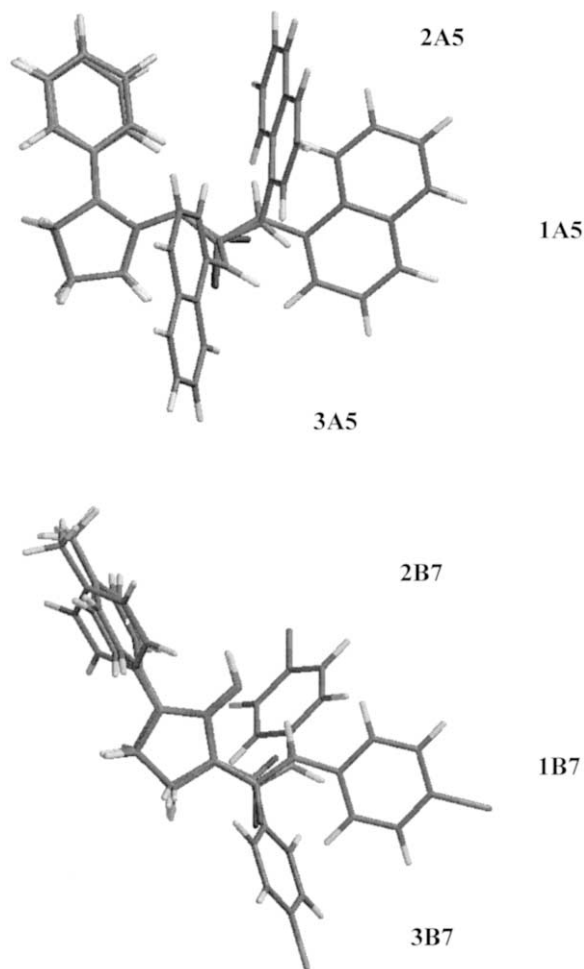


Figure 13. Fit of the calculated conformers **1**, **2** and **3** of compounds **A5** and **B7** (by the three nitrogen atoms of the guanidine moiety).

molecules can adopt the structure of conformer **2** and act as a competitive antagonist against molecules in conformation **1**.

In conclusion the results of our investigation lead to the finding of a new group of 1-aryl-2-iminoimidazolidine derivatives containing the urea moiety showing affinity toward opioid (μ), serotonin (5-HT₂) and benzodiazepin (BZD) receptors. The opioid activity confirmed by both the behavioural and binding affinity tests and the structural analyses of the energetically preferable conformers allowed the formulation of the non-classical pharmacophor hypothesis of the μ receptor activation based on the respective location of the two hydrophobic and one H-bond acceptor sites. The results obtained can be a starting point for the further investigation in the search for new, and more selective opioid receptors' ligands of an atypical structure, e.g. deprived of the basic centre. They can also possibly lead to the finding of the new groups of compounds active in the opioid system with less or no side effects typically known so far.

6. Experimental protocols

6.1. Chemical analysis

Chemicals (isocyanates) were obtained from Merck as 'synthesis grade' chemicals and used without further purification. Melting points (m.p. (dec)) were determined on a Boetius apparatus and are given uncorrected. NMR spectra (¹H and ¹³C) were recorded on Varian Gemini 200 MHz and Bruker 200 MHz spectrometers in D₆-DMSO with TMS as an external standard at 295 K. IR spectra were recorded on infrared Fourier spectrometer STIR as KBr pellets. TLC was performed on commercial Merck SiO₂ 60 F₂₅₄ plates with chloroform–methanol (4:1) (**I**) and benzene–ethyl ether (8:1) (**II**) eluent systems, visualisation: UV light $\lambda = 254$ and 355 nm. Flash chromatography was performed on commercial silica-gel 60–200 mesh (Merck) in a glass column (45×250 mm) with eluent system (**II**). Elemental analyses were performed on a Perkin–Elmer analyser and were in the range of $\pm 0.4\%$ for each element analysed (C, H, N, Cl).

6.1.1. Synthesis of 1-(1-arylimidazolidine-2-ylidene)-3-arylureas (series **A**) and 1-aryl-2-imine-3-arylaminocarbonylimidazolidines (series **B**) (general procedure)

Free base (0.05 mol) of 1-aryl-2-aminoimidazolidine-2 was dissolved in 150 mL of methylene chloride and

added to the solution of 0.05 mol of arylisocyanate in 100 mL of methylene chloride. The mixture was shaken for 1 h in room temperature (r.t.) and left for 5 h in the same temperature. Solvent was removed by distillation and the rubber-like residue was treated with warm 2-propanol (a), mixture of 2-propanol and acetone (4:1) (b) or 2-propanol and ethyl acetate (5:1) (c) until the white precipitation was obtained. Solid was separated by suction.

Crude reaction product (1 g) was introduced to the front of the column and eluted with 1000 mL of the eluent system II at 10 mL min⁻¹, collecting 10 mL fractions. The fractions were checked by TLC for the presence of single isomer, collected together and the solvent was removed by low pressure evaporation. The residue obtained was crystallised from 2-propanol (series B) or DMF–2-propanol mixture (series A).

6.2. Crystallographic analysis

Diffraction data for 1-(1-phenylimidazolidine-2-ylidene)-3-(4-chlorophenyl)urea (**A2**) were measured on a Siemens P3 diffractometer using variable scan speed (ω - 2θ scan mode) and graphite monochromated Mo K α radiation ($\lambda = 0.71073$ Å). A single crystal of dimensions 0.35×0.32×0.25 mm was used at ambient temperature. The crystal was triclinic, space group $P\bar{1}$; $a = 10.624(2)$ Å, $b = 11.0851(2)$ Å, $c = 13.466(2)$ Å, $\alpha = 79.58(1)^\circ$, $\beta = 80.10(1)^\circ$, $\gamma = 77.73(1)^\circ$, $V = 1409.3(5)$ Å³, $Z = 4$, $d_{\text{calc}} = 1.385$ g cm⁻³. Up to $\theta_{\text{max}} = 27.54^\circ$, 7359 reflections were collected, of which 6982 were independent reflections [$R_{\text{(int)}} = 0.0104$] were used in the calculations. The data set was corrected for absorption ($\mu = 0.26$ mm⁻¹) and extinction ($\kappa = 0.028(2)$) effects. Crystal structure was solved by the direct method using SHELXS-97 [14] program and refined by full-matrix least-squares on F^2 using the SHELXL-97 [15] program. The non-hydrogen atoms were refined with anisotropic displacement parameters. Positions of H-atoms were calculated from the geometry assuming the trigonal or tetrahedral configuration of the respective non-H atoms. H-atoms were given isotropic factors of 1.2 U_{eq} of the bonded C–N-atoms and the ‘riding’ model was used in the refinement. The final discrepancy factors are $R_1 = 0.044$, $wR_2 = 0.114$ for $I > 2\sigma(I)$, and $R_1 = 0.055$, $wR_2 = 0.121$ for all data, $S = 1.045$.

The lists of atomic coordinates, displacement parameters and complete geometry have been deposited at the Cambridge Crystallographic Data Centre (file No. CCDC 166 896).

6.3. Pharmacological analysis

6.3.1. Behavioural tests

6.3.1.1. Materials and methods

The experiments were performed on male Albino Swiss mice (18–30 g). Animals, 8–10 per cage, were kept at room temperature (20 ± 1 °C), on a 12/12 h dark–light cycle. Standard food (Bacutil, Motycz, Poland) and water were available ad libitum. The substances investigated (**A2**, **A3**, **A5**, **A7**, **A8** and **B7**) were administered intraperitoneally (i.p.) as suspensions in aqueous solution of 0.5% methylcellulose (tylose). The compounds were injected 60 min before the test. The controls received an equivalent volume of the solvent.

The acute toxicity of the compounds was assessed in mice according to the Litchfield and Wilcoxon [16] method as LD₅₀ calculated based on mortality within 48 h. In addition, the activity of the compounds was assessed in the following tests.

Locomotor activity was measured in photoresistor actometer for a single mouse for 30 min as: (a) spontaneous activity; and (b) amphetamine-induced hyperactivity—mice received subcutaneously (s.c.) 5 mg kg⁻¹ of amphetamine 30 min before the test.

Nociceptive reactions were studied in: (a) the ‘hot plate’ test (56 °C) described by Eddy and Leimbach [17]—the test was carried out 60 min before and 30, 60, 90 and 120 min after the compounds were administered; (b) the acetic acid (0.6%) induced ‘writhing’ test [18]—the number of writhing episodes was measured for 10 min starting 5 min after the i.p. administration of the acid solution.

Hexobarbital (65 mg kg⁻¹)—induced narcosis was recorded as the time elapsing between the loss and recovery of the righting reflex.

Motor coordination was evaluated in the rota-rod test [19].

Body temperature in normothermic mice was measured in the rectum by means of thermistor thermometer.

Pentylentetrazole (110 mg kg⁻¹, s.c.)—induced convulsions were evaluated as the number of mice clonic seizures, tonic convulsions and dead animals.

‘Head twitch’ responses after 5-hydroxytryptophan (5-HTP), according to Corne et al. [20]. Mice received 5-HTP (180 mg kg⁻¹, i.p.) and the number of head twitches was recorded in six 2 min intervals (4–6, 14–16, 24–26, 34–36, 44–46, 54–56 min).

Influence of naloxone (5 mg kg⁻¹, s.c.) on the antinociceptive effect of the compounds tested was assessed in the writhing test.

The compounds were injected in doses equivalent to 0.1, 0.05, 0.025 and 0.0125 LD₅₀ (200, 100, 50 and 25 mg kg⁻¹, respectively).

Statistics. The data obtained were calculated by Student's *t*-test and chi square test with Yates correction (pentylene-tetrazole-induced seizures).

6.3.2. Binding assays

The affinity of **A5** and **B7** compounds toward opioid (μ), serotonin (5-HT₂) and benzodiazepine (BDZ) receptor was investigated by the radioligand displacement method. The radioligands [³H]-Flunitrazepam (specific activity 81 Ci mmol⁻¹), [³H]-Ketanserin (specific activity 63.7 Ci mmol⁻¹) and [³H]-Naloxone (specific activity 52 Ci mmol⁻¹) were purchased from Amersham. In all experiments the samples were counted for radioactivity in a Beckman LS 3801 scintillation counter. The specific binding was defined as the difference between the total and unspecific binding. EC₅₀ was estimated using GraphPad Prism computer program.

6.3.2.1. Displacement of ³H-naloxone (52 Ci mmol⁻¹) by investigated compounds

Tissues (cerebral cortex) from individual naive animals were processed separately. They were homogenised at 0 °C in 20 volumes of 50 mmol L⁻¹ Tris-HCl buffer, pH 7.6. The homogenate was centrifuged at 0 °C and 25 000g for 30 min, and the pellet was rehomogenised and incubated in a shaking water bath at 37 °C for 45 min (preincubation), and then recentrifuged at 0 °C and 25 000g for 30 min. The pellet (fraction P₁+P₂) was stored at -20 °C for no longer than 48 h. For incubation it was reconstituted in 20 volumes of the incubation buffer pH 7.6. The incubation mixture contained 100 mmol L⁻¹ NaCl, the final volume 550 μ L contained 450 μ L membrane suspension, 50 μ L ³H-naloxone solution (2.5 nmol) and 50 μ L buffer containing seven concentrations (1 nmol–100 μ mol) of the compounds investigated (**A5** and **B7**). For measuring the unspecific binding, naloxone in a final concentration of 10 μ mol was used. The incubation was carried out in duplicates, in a shaking water bath, at 30 °C for 30 min. The addition of the radioligand initiated the incubation, which was terminated by rapid filtration through GF/C Whatman fibreglass filters. The filters were then rinsed twice with 5 mL portions of ice-cold incubation buffer and were placed in plastic scintillation minivials. Scintillation fluid

(3 mL) was added, and the samples were counted for radioactivity.

6.3.2.2. Displacement of ³H-Ketanserin (63.7 Ci mmol⁻¹) by the compounds investigated

Tissues (structures) from individual naive animals were processed separately. They were homogenised at 0 °C in 20 volumes of 50 mmol L⁻¹ Tris-HCl buffer, pH 7.6. The homogenate was centrifuged at 0 °C and 25 000g for 15 min, and then the pellet was rehomogenised and incubated in a shaking water bath at 37 °C during 15 min. (preincubation), and then recentrifuged at 0 °C and 25 000g for 30 min. After decanting the supernatant, the pellet (fraction P₁+P₂) was stored at -20 °C for no longer than 48 h. For incubation it was reconstituted in 20 volumes of the incubation buffer pH 7.6. The incubation mixture (final volume 550 μ L) consisted of 450 μ L membrane suspension, 50 μ L ³H-ketanserin solution (0.6 nmol) and 50 μ L buffer containing seven concentrations (1 nmol–100 μ mol) of the compounds investigated (**A5** and **B7**). For measuring unspecific binding, cold ketanserin in a final concentration of 10 μ mol was used. The incubation was carried out in duplicates, in a shaking water bath, at 37 °C for 20 min. The addition of the radioligand initiated the incubation, which was terminated by rapid filtration through GF/C Whatman fibreglass filters. The filters were then rinsed twice with 5 mL portions of ice-cold incubation buffer and were placed in plastic scintillation minivials. Scintillation fluid (3 mL) was added, and the samples were counted for radioactivity.

6.3.2.3. Displacement of ³H-Flunitrazepam (81 Ci mmol⁻¹) by the compounds investigated

Tissues from individual naive animals were processed separately. They were homogenised at 0 °C in 20 volumes of 50 mmol L⁻¹ Tris-HCl buffer, pH 7.6. The homogenate was centrifuged at 0 °C and 1000g for 15 min, and then recentrifuged at 0 °C and 25 000g for 30 min. After decanting the supernatant, the pellet (fraction P₂) was stored at -20 °C for no longer than 48 h. For incubation it was reconstituted in 20 volumes of the incubation buffer pH 7.6. The incubation mixture (final volume 550 μ L) consisted of 450 μ L membrane suspension, 50 μ L ³H-flunitrazepam solution (2 nmol) and 50 μ L buffer containing seven concentrations (1 nmol–100 μ mol) of the compounds investigated (**A5** and **B7**). For measuring the unspecific binding, cold diazepam in a final concentration of 10 μ M was used. The incubation was carried out in duplicates, in a shaking water bath, at

0 °C for 60 min. The addition of the radioligand initiated the incubation, which was terminated by rapid filtration through GF/C Whatman fibreglass filters. The filters were then rinsed twice with 5 mL portions of ice-cold incubation buffer and were placed in plastic scintillation minivials. Scintillation fluid (3 mL) was added, and the samples were counted for radioactivity.

References

- [1] Bowman W.C., Rand M.J. (Eds.), Textbook of Pharmacology, Blackwell, London, 1980 (chap. 16).
- [2] Korlipara V.L., Takemori A.E., Portoghese P.S., J. Med. Chem. 38 (1995) 1337.
- [3] Mosberg H.I., Omnaas J.R., Lomize A.L., Heyl D.L., Nordan L., Mousigian C., Davis P., Porreca F., J. Med. Chem. 37 (1994) 4384.
- [4] Huang P., Kim S., Loew G., J. Comput.-Aided Mol. Des. 11 (1997) 21–28.
- [5] Matosiuk D., Tkaczyński T., Stefańczyk J., Acta Pol. Pharm. 53 (1996) 209–212.
- [6] Knoevenagel E., Mercklin E., Ber 37 (1904) 4089–4092.
- [7] Takeda A., J. Org. Chem. 22 (1957) 1096–1099 (and other references there).
- [8] Lehman D., Faust G., DD 155 614I (1982); Chem. Abs. 98 (1983) 125599g.
- [9] Matosiuk D., Tkaczyński T., Jagiełło-Wójtowicz E., Wielosz M., Szurska G., Chodkowska A., Janusz W., Kleinrok Z., Pol. J. Pharmacol. Pharm. 44 (1992) 307–312.
- [10] Graham L.P., An Introduction to Medicinal Chemistry, Oxford University Press, New York, 1995 (chap. 12).
- [11] North P.C., in: King F.D. (Ed.), Medicinal Chemistry: Principles and Practice, Royal Society of Chemistry, Cambridge, 1994 (chap. 18).
- [12] Glennon R.A., Dukat M., Serotonin receptor subtypes, in: Bloom F.E., Kupfer D.J. (Eds.), Psychopharmacology: The Fourth Generation of Progress, Raven Press, New York, 1995, pp. 415–429.
- [13] PC Spartan Pro v. 1.05, Wavefunction, Irving, CA, USA, 2000.
- [14] Sheldrick G.M., SHELXS-97, Program for Crystal Structure Solution, University of Göttingen, Göttingen, Germany, 1997.
- [15] Sheldrick G.M., SHELXL-97, Program for Crystal Structure Refinement, University of Göttingen, Göttingen, Germany, 1997.
- [16] Litchfield L.T., Wilcoxon F., J. Pharmacol. Exp. Ther. 96 (1949) 99–113.
- [17] Eddy N.B., Leimbach D., J. Pharmacol. Exp. Ther. 107 (1953) 385–393.
- [18] Koster R., Anderson M., DeBeer E.J., Fed. Proc. 18 (1959) 412–415.
- [19] Gross F., Tripod J., Meir R., Schweiz. Med. Wochschr. 85 (1955) 305–309.
- [20] Corne S.J., Pickering R.W., Werner B.T., Br. J. Pharmacol. 20 (1963) 106–120.